HHS Public Access

Author manuscript

Mol Cancer Ther. Author manuscript; available in PMC 2019 March 01.

Published in final edited form as:

Mol Cancer Ther. 2018 March ; 17(3): 661–670. doi:10.1158/1535-7163.MCT-17-0851.

Molecularly Targeted Cancer Combination Therapy with Near Infrared Photoimmunotherapy and Near Infrared Photo-release with Duocarmycin-antibody Conjugate

Tadanobu Nagaya[1], **Alexander P. Gorka**[2], **Roger R. Nani**[2], **Shuhei Okuyama**[1], **Fusa Ogata**[1], **Yasuhiro Maruoka**[1], **Peter L. Choyke**[1], **Martin J. Schnermann**[2], and **Hisataka Kobayashi**[1,*]

[1]Molecular Imaging Program, Center for Cancer Research, National Cancer Institute, National Institutes of Health, Bethesda, Maryland, 20892, United States of America

[2]Chemical Biology Laboratory, Center for Cancer Research, National Cancer Institute, Frederick, Maryland, 21702, United States of America

Abstract

Near infrared photoimmunotherapy (NIR-PIT) is a highly selective tumor treatment that employs an antibody-photo-absorber conjugate (APC). However, the effect of NIR-PIT can be enhanced when combined with other therapies. NIR photocaging groups, based on the heptamethine cyanine scaffold, have been developed to release bioactive molecules near targets after exposure to light. Here, we investigated the combination of NIR-PIT employing panitumumab-IR700 (pan-IR700) and the NIR-releasing compound, CyEt-Panitumumab-Duocarmycin (CyEt-Pan-Duo). Both pan-IR700 and CyEt-Pan-Duo showed specific binding to the EGFR-expressing MDAMB468 cell line *in vitro*. In *in vivo* studies, additional injection of CyEt-Pan-Duo immediately after NIR light exposure resulted in high tumor accumulation and high tumor-background ratio. To evaluate the effects of combination therapy *in vivo*, tumor-bearing mice were separated into 4 groups: (1) control; (2) NIR-PIT; (3) NIR-release; (4) combination of NIR-PIT and NIR-release. Tumor growth was significantly inhibited in all treatment groups compared with the control group ($p < 0.05$), and significantly prolonged survival was achieved ($p < 0.05$ vs control). The greatest therapeutic effect was shown with NIR-PIT and NIR-release combination therapy. In conclusion, combination therapy of NIR-PIT and NIR-release enhanced the therapeutic effects compared with either NIR-PIT or NIR-release therapy alone.

Keywords

near infrared photoimmunotherapy; near infrared release; duocarmycin; SUPR; photocaging

*Corresponding author: Hisataka Kobayashi, M.D., Ph.D., Molecular Imaging Program/NCI/NIH, Bldg. 10, Rm. B3B69, 10 Center Dr., Bethesda MD, 20892-1088 USA, Phone: 301-435-4086; Fax: 301-402-3191; kobayash@mail.nih.gov.

Potential Conflicts of Interest

No potential conflicts of interest were disclosed.

Introduction

Near infrared photoimmunotherapy (NIR-PIT) is a newly developed cancer treatment that employs a highly targeted monoclonal antibody (mAb)-photo-absorber conjugate (APC). The photo-absorber, IRDye700DX (IR700, silica-phthalocyanine dye), is a highly hydrophilic dye, differentiating it from prior hydrophobic dyes used in photo dynamic therapy (PDT) (1). Therefore, mAb-IR700 conjugates behave in the body similar to non-conjugated antibodies. Once the APC is injected and time elapses to allow sufficient binding to target cells, exposure to NIR light results in rapid cell swelling, leading to cell membrane rupture and extrusion of cell contents into the extracellular space. Cell death after NIR-PIT is characterized as necrotic/immunogenic cell death (2). A first-in-human phase 1 trial of epidermal growth factor receptor (EGFR) targeted NIR-PIT in patients with inoperable head and neck cancer was initiated in June 2015 (https://clinicaltrials.gov/ct2/show/NCT02422979) and has recently advanced to phase 2.

A unique advantage of NIR-PIT is that it leads to immediate increases in vascular permeability of treated tumors which can result in 10- to 24-fold enhancement of macromolecules or nano-drugs delivery. This phenomenon has been termed super enhanced permeability and retention (SUPR) effects because it is substantially greater than conventional “enhanced permeability and retention (EPR)” which is commonly seen in untreated tumors (3–5). SUPR effects result in homogeneous redistribution of already circulating APC or reinjected APCs or other nano-sized agents in treated tumors, at least partly overcoming baseline heterogeneity in drug delivery commonly observed in untreated tumors. Therefore, additional exposures of NIR-light can further improve therapeutic effects by depositing additional APCs in the tumor bed after initial NIR-PIT (5, 6). To achieve superior NIR-PIT therapeutic effects, repeated NIR light exposures with one APC or a combination of NIR-PIT and nano-sized anticancer drugs have been successfully demonstrated (5, 7).

Light in the NIR range (650 - 900 nm) has several advantages over visible light. NIR light can penetrate deeper into tissue while carrying minimal toxicity. As a consequence, NIR dyes have been employed in both diagnostic and therapeutic applications in preclinical and clinical settings (8, 9).

NIR photocaging groups, based on the heptamethine cyanine scaffold, bound to a targeting moiety, and have the ability to accumulate in targeted tissue, enabling both diagnosis by fluorescence imaging and therapy by releasing potent bioactive molecules after NIR light exposure (10–13). Uncaging reactions that are induced with NIR light could site-specifically deliver bioactive compounds to any part of the body. The development of efficient uncaging reactions triggered by the modest photonic energy of NIR light represents a significant chemical challenge and is the subject of ongoing study (14, 15). The most advanced molecule in this area, CyEt-Panitumumab-Duocarmycin degree of labeling 4 (CyEt-Pan-Duo), releases a derivative of the DNA-alkylating natural product, duocarmycin. This duocarmycin-antibody conjugate shows light-dependent cytotoxic activity in the picomolar range and can be activated with clinically achievable doses of NIR light (16). Studies in mouse models showed that the conjugate was well tolerated, was readily visible with

fluorescence imaging, and showed significant antitumor efficacy following external therapeutic doses of NIR light exposure (16).

Superior delivery of target molecules into target tumors prior to NIR-release could enhance therapeutic effects. When combination therapy with pan-IR700 and CyEt-Pan-Duo is employed, there is both a large increase in delivered dose and a more homogeneous distribution of CyEt-Pan-Duo based on the SUPR effect after initial NIR-PIT. Thus, a potential strategy is to treat a tumor with conventional NIR-PIT followed by exposure to another dose of NIR to release duocarmycin as an adjuvant therapy. In this study, we investigate the *in vivo* distribution of CyEt-Pan-Duo after NIR-PIT. Following this, NIR-PIT and NIR-release were performed separately and in combination in a tumor bearing mouse model *in vivo* and therapeutic efficacy was established.

Materials and Methods

Reagents

Water soluble, silica-phthalocyanine derivative, IRDye 700DX NHS ester was obtained from LI-COR Biosciences (Lincoln, NE, USA). Panitumumab, a fully humanized clinical IgG_2 mAb directed against EGFR, was purchased from Amgen (Thousand Oaks, CA, USA). All other chemicals were of reagent grade.

Synthesis of IR700 conjugated panitumumab

Conjugation of dyes with mAb was performed according to a previous report (1). In brief, panitumumab (1.0 mg, 6.8 nmol) was incubated with IR700 NHS ester (60.2 μg, 30.8 nmol) in 0.1 M Na_2HPO_4 (pH 8.6) at room temperature for 1 h. The mixture was purified with a Sephadex G25 column (PD-10; GE Healthcare, Piscataway, NJ, USA). The protein concentration was determined with Coomassie Plus protein assay kit (Thermo Fisher Scientific Inc, Rockford, IL, USA) by measuring the absorption at 595 nm with UV-Vis (8453 Value System; Agilent Technologies, Santa Clara, CA, USA). The concentration of IR700 was measured by absorption at 689 nm to confirm the number of fluorophore molecules per mAb. The synthesis was controlled so that an average of two IR700 molecules was bound to a single antibody. We abbreviate IR700 conjugated to panitumumab as pan-IR700.

Synthesis of Cyanine-Caged Duocarmycin conjugated panitumumab

Synthesis is described in a previous report (16). Following synthesis, cyanine-caged duocarmycin was conjugated to panitumumab using conventional conditions (pH 8.5 phosphate buffered saline, PBS, buffer) with 4.5 equivalent of the small molecule and purified using preparative size-exclusion chromatography (SEC) to provide CyEt-Panitumumab-Duocarmycin degree of labeling degree 4 (CyEt-Pan-Duo). Absorbance of the conjugate was also measured using UV-Vis.

SDS-PAGE

As a quality control for conjugates, we performed sodium dodecyl sulfate-polyacrylamide gel electrophoresis (SDS-PAGE). Conjugate was separated by SDS-PAGE with a 4-20%

gradient polyacrylamide gel (Life Technologies, Gaithersburg, MD, USA). A standard marker (Crystalgen Inc., Commack, NY, USA) was used as a protein molecular weight marker. After electrophoresis at 80 V for 2.5 h, the gel was imaged with a Pearl Imager (LI-COR Biosciences, Lincoln, Nebraska, USA) using the 700 nm and 800 nm fluorescence channels. We used diluted panitumumab as a control. The gel was stained with Colloidal Blue staining to determine the molecular weight of conjugate.

Cell culture

EGFR-expressing MDAMB468-luc (human breast cancer) cells, which are stably transduced luciferase-transfected cells were used in this study (17, 18). High luciferase expression was confirmed with 10 passages. Cells were grown in RPMI 1640 (Life Technologies, Gaithersburg, MD, USA) supplemented with 10% fetal bovine serum and 1% penicillin/streptomycin (Life Technologies) in tissue culture flasks in a humidified incubator at 37°C in an atmosphere of 95% air and 5% carbon dioxide.

Flow cytometry

To verify *in vitro* pan-IR700 and CyEt-Pan-Duo binding, fluorescence from cells after incubation with APC was measured using a flow cytometer (FACS Calibur, BD BioSciences, San Jose, CA, USA) and CellQuest software (BD BioSciences). MDAMB468-luc cells (2×10^5) were seeded into 12 well plates and incubated for 24 h. Medium was replaced with fresh culture medium containing 3 μg/mL of pan-IR700 or CyEt-Pan-Duo and incubated for 6 h at 37°C. After washing with PBS, PBS was added. A 488-nm argon ion laser was used for excitation. Signals from cells were collected with a 653-669 nm band-pass filter.

Fluorescence microscopy

Ten thousand MDAMB468-luc cells were seeded on cover-glass-bottomed dishes and incubated for 24 h. Pan-IR700 or CyEt-Pan-Duo was then added to the culture medium at 3 μg/mL and incubated for 6 h at 37°C. After incubation, the cells were washed with PBS. To detect the antigen specific localization, fluorescence microscopy was performed (BX61; Olympus America, Inc., Melville, NY, USA) equipped with the following filters: excitation wavelength 590-650 nm and 672.5-747.5 nm, emission wavelength 665-740 nm and 765-855 nm for pan-IR700 and CyEt-Pan-Duo, respectively. Transmitted light differential interference contrast (DIC) images were also acquired.

In vitro treatment effect of combination therapy with NIR-PIT and NIR-release

MDAMB468-luc cells (2×10^5) were placed in 12 well plates and incubated for 24 h. Medium was replaced with fresh culture medium. Cells were divided into 8 groups of at least 3 wells per group for the following treatments: (1) no treatment (control); (2) NIR light exposure only without conjugate (NIR light); (3) 6 μg/mL of pan-IR700 (pan-IR700); (4) 6 μg/mL of CyEt-Pan-Duo (CyEt-Pan-Duo); (5) 3 μg/mL of pan-IR700 and 3 μg/mL of CyEt-Pan-Duo (pan-IR700 + CyEt-Pan-Duo); (6) 6 μg/mL of CyEt-Pan-Duo, NIR light exposure was administered at 6 J/cm^2 (CyEt-Pan-Duo + NIR light); (7) 6 μg/mL of pan-IR700, NIR light exposure was administered at 6 J/cm^2 (pan-IR700 + NIR light); (8) 3 μg/mL of pan-

IR700 and 3 μg/mL of CyEt-Pan-Duo, NIR light exposure was administered at 6 J/cm^2 (pan-IR700 + CyEt-Pan-Duo + NIR light). Conjugates were incubated for 6 h at 37°C. After washing with PBS, phenol red free medium was added. Cells were irradiated with a red light-emitting diode (LED), which emits light at 690 ± 20nm wavelength (L690-66-60; Marubeni America Co., Santa Clara, CA, USA) at a power density of 50 mW/cm^2 as measured with an optical power meter (PM 100, Thorlabs, Newton, NJ, USA). To verify *in vitro* therapeutic effect of combination therapy, cell count was measured using an automated cell counter (Countess™, Invitrogen, Carlsbad, CA, USA) 24 h after treatment.

Animal and tumor models

All *in vivo* procedures were conducted in compliance with the Guide for the Care and Use of Laboratory Animal Resources (1996), US National Research Council, and approved by the local Animal Care and Use Committee. Six to eight week old female homozygote athymic nude mice were purchased from Charles River (NCI-Frederick, Frederick, MD, USA). During the procedure, mice were anesthetized with inhaled 3-5% isoflurane and/or via intraperitoneal injection of 1 mg of sodium pentobarbital (Nembutal Sodium Solution, Ovation Pharmaceuticals Inc., Deerfield, IL, USA). In order to determine tumor volume, the greatest longitudinal diameter (length) and the greatest transverse diameter (width) were measured with an external caliper. Tumor volumes were based on caliper measurements and were calculated using the following formula; tumor volume = length × width^2 × 0.5. Body weight was also measured. Mice were monitored daily for their general health including observation of skin color, weight loss or loss of appetite. Tumor volumes were measured two times a week until the tumor volume reached 2000 mm^3, whereupon the mice were euthanized with inhalation of carbon dioxide gas.

In vivo 800 nm fluorescence imaging studies using CyEt-Pan-Duo

MDAMB468-luc cells (6 × 10^6) were injected subcutaneously in the right dorsum of the mice. Tumors were studied after they reached volumes of approximately 50 mm^3. To evaluate *in vivo* CyEt-Pan-Duo biodistribution after NIR-PIT, tumor-bearing mice were randomized into 2 groups of at least 10 animals per group for the following treatments: (1) 100 μg of CyEt-Pan-Duo was injected on day 1 after 100 μg of pan-IR700 i.v., no NIR light was administered (CyEt-Pan-Duo); (2) NIR light was administered at 50 J/cm^2 on day 1 after 100 μg of pan-IR700 i.v., 100 μg of CyEt-Pan-Duo was injected immediately after NIR exposure (NIR-PIT + CyEt-Pan-Duo). Tumors were irradiated with a LED. Serial dorsal fluorescence images of CyEt-Pan-Duo were obtained with a Pearl Imager using a 800 nm fluorescence channel before and 0, 1, 3, 6, 9, and 24 hours after i.v. injection of 100 μg of CyEt-Pan-Duo via the tail vein. Pearl Cam Software (LICOR Biosciences, Lincoln, NE, USA) was used for analyzing fluorescence intensities. Region of interests (ROIs) were placed on the tumor. ROIs were also placed in the adjacent non-tumor region as background (left dorsum). Average fluorescence intensity of each ROI was calculated. Tumor background ratios (TBRs = fluorescence intensities of target/fluorescence intensities of background) were also calculated (n = 10).

In vivo treatment effect of combination therapy with NIR-PIT and NIR-release

Next, to clarify the *in vivo* treatment effect of NIR-release with conventional NIR-PIT we performed combination therapy. MDAMB468-luc cells (6×10^6) were injected subcutaneously in the right dorsum of the mice. Tumors were studied after they reached volumes of approximately 50 mm^3. To examine the therapeutic effect of *in vivo* combination therapy with NIR-PIT and NIR-release, tumor-bearing mice were randomized into 4 groups of at least 10 animals per group for the following treatments: (1) no treatment (control); (2) 100 μg of pan-IR700 i.v., NIR light was administered at 50 J/cm^2 on day 1 and 100 J/cm^2 on day 2 after injection (NIR-PIT); (3) NIR light was administered at 50 J/cm^2 on day 1 without pan-IR700 and 100 μg of CyEt-Pan-Duo was injected immediately after NIR exposure, then NIR light was administered at 100 J/cm^2 on day 2 (NIR-release); (4) 100 μg of pan-IR700 i.v., NIR light was administered at 50 J/cm^2 on day 1 and 100 μg of CyEt-Pan-Duo was injected immediately after NIR exposure, then NIR light was administered at 100 J/cm^2 on day 2 (NIR-PIT + NIR-release). Tumors were irradiated with a LED. Serial fluorescence images, as well as white light images, were obtained using a Pearl Imager with 700 nm and 800 nm fluorescence channel.

In vivo bioluminescence image

For *in vivo* bioluminescence imaging (BLI), D-luciferin (15 mg/mL, 200 μL) (Gold Biotechnology, St. Louis, MO, USA) was injected intraperitoneally and the mice were analyzed on a BLI system (Photon Imager; Biospace Lab, Paris, France) for luciferase activity (photons/min). ROIs were set on the entire tumors to quantify the luciferase activities. ROIs were also placed in the adjacent non-tumor region as background. Average luciferase activity of each ROI was calculated using M3 Vision Software (Biospace Lab). To measure relative therapeutic effect, luciferase activity of the tumor before NIR-PIT set to 100%.

Statistical analysis

Data are expressed as means ± standard error of mean (SEM). Statistical analyses were carried out using GraphPad Prism version 7 (GraphPad Software, La Jolla, CA, USA). For multiple comparisons, a one-way analysis of variance (ANOVA) followed by the Tukey's correction for multiple comparisons was used. The cumulative probability of survival based on volume (2000 mm^3) was estimated in each group with a Kaplan-Meier survival curve analysis, and the results were compared using the Gehan-Breslow-Wilcoxon test. Mann-Whitney-U test was used to compare the fluorescence intensities and TBRs to controls. A p-value of < 0.05 was considered statistically significant.

Results

Characterization of pan-IR700 and CyEt-Pan-Duo on MDAMB468-luc cell

To characterize both conjugates, each absorbance spectrum was analyzed using UV-Vis (Supplementary Fig. 1) to show that conjugation ratios of both pan-IR700 and CyEt-Pan-Duo Ab-conjugates are identical as ones which we previously reported (1, 16). As defined by SDS-PAGE, pan-IR700, CyEt-Pan-Duo and non-conjugated control panitumumab

showed a nearly identical molecular weight. Fluorescence was seen in the band containing both pan-IR700 and CyEt-Pan-Duo but not the others (Fig. 1A). SEM of CyEt-Pan-Duo consistent with previous report (16). After a 6 h incubation with either pan-IR700 or CyEt-Pan-Duo, MDAMB468-luc cells demonstrated fluorescence signal, which was confirmed with flow cytometry (Fig. 1B) and fluorescence microscopy (Fig. 1C).

In vitro therapeutic effect of combination therapy with NIR-PIT and NIR-release

Based on survived cell counts, both Ab-conjugates bound to target MDAMB468 cells and induced strong cytotoxicity only after exposure of NIR light (NIR-release, NIR-PIT and combination with NIR-PIT and NIR-release, see Fig. 1D). The combination therapy using both conjugates showed at least additive on-target toxicity. Additionally, mild cell death was observed in CyEt-Pan-Duo alone and pan-IR700 + CyEt-Pan-Duo even without NIR light exposure. In contrast, no treatment effect was shown in NIR light only and pan-IR700 only groups.

In vivo 800 nm fluorescence imaging studies using CyEt-Pan-Duo

The treatment and imaging regimen is shown in Fig. 2A. 800 nm fluorescence was rapidly seen in tumors undergoing NIR-PIT + CyEt-Pan-Duo tumors (Fig. 2B and 2C). On the other hand, tumors receiving only CyEt-Pan-Duo showed a gradual increase in 800nm fluorescence (Fig. 2B and 2C). Because of the SUPR effect, CyEt-Pan-Duo was able to leak into the tumors more rapidly and the 800 nm fluorescence intensities were significantly higher in the NIR-PIT + CyEt-Pan-Duo group compared to CyEt-Pan-Duo-only group at the most time points ($p < 0.01$ at 1, 3, 6, and 9 hour, $p < 0.05$ at 24 hour) (Fig. 2C). TBR increased gradually within 1 day in both CyEt-Pan-Duo only tumors and NIR-PIT + CyEt-Pan-Duo tumors (Fig. 2D). TBRs were also significantly higher in NIR-PIT + CyEt-Pan-Duo group compared to CyEt-Pan-Duo only group at all time points ($p < 0.01$).

In vivo treatment effect of combination therapy with NIR-PIT and NIR-release using luciferase activity

The treatment and imaging regimen is shown in Fig. 3A. One day after injection of pan-IR700 followed by NIR-PIT, the tumors had persistently reduced luciferase activity (Fig. 3B). All treatment (NIR-PIT, NIR-release, and NIR-PIT + NIR-release) resulted in decreases in bioluminescence compared with control (Fig. 3B). Luciferase activity significantly decreased after the all treatment groups ($p < 0.01$ vs. control group) (Fig. 3C). In contrast, luciferase activity of tumor in control group showed an increase due to rapid tumor growth.

In vivo treatment effect of combination therapy with NIR-PIT and NIR-release

The treatment and imaging regimen is shown in Fig. 4A. One day after injection of pan-IR700, the tumors showed higher IR700 fluorescence intensity than did the tumor with no pan-IR700 injection. After exposure to 50 J/cm^2 of NIR light, pan-IR700 tumor fluorescence signal decreased due to dying cells and partial photo-bleaching (Fig. 4B). One day after injection of CyEt-Pan-Duo, the tumors in NIR-PIT + NIR-release group showed higher CyEt-Pan-Duo fluorescence intensity than did the tumor in NIR-release only group (Fig.

4B). Immediately after exposure to 100 J/cm^2 of NIR light, CyEt-Pan-Duo fluorescence signal strongly decreased due to photo-release. After photo-release, CyEt-Pan-Duo fluorescence signal gradually increased in both the NIR-release group and the NIR-PIT + NIR-release group, however, the accumulation of CyEt-Pan-Duo was higher in NIR-PIT + NIR-release tumors compared with NIR-release only tumor. Tumor growth was significantly inhibited in all treatment groups compared with the control group ($p < 0.001$) (Fig. 4C). Tumor growth in the NIR-PIT + NIR-release group was significantly reduced compared with the NIR-release only group ($p < 0.01$). Significantly prolonged survival was also achieved in all treatment groups compared with the control group ($p < 0.05$ for NIR-release group, $p < 0.01$ for NIR-PIT group and NIR-PIT + NIR-release group) (Fig. 4D). Survival of the NIR-PIT group was significantly prolonged compared with the NIR-release only group ($p < 0.01$). Furthermore, significantly prolonged survival was also achieved in NIR-PIT + NIR-release group compared with NIR-PIT-alone group ($p < 0.05$). From these results, maximal effects were shown with the combination of NIR-PIT and NIR-release. There was no skin necrosis or toxicity attributable to the treatment in any group.

Discussion

In oncology, mAbs have favorable pharmacokinetics for tumor targeting because of their stable binding to target molecules that leads to high TBRs. However, a limitation of mAb-based therapy is inhomogeneous intra-tumoral distribution of the antibodies due to their relatively large molecular size (19–21). This occurs especially when a mAb has a high binding affinity for the target receptor and/or the tumor cells express high levels of target antigens. In these cases, mAbs are saturated on the most bioavailable antigen-positive cells which are typically located in the immediate perivascular space. This “binding site barrier” effectively hampers the penetration of mAbs deeper into the tumor (22–25). To achieve sufficient therapeutic effects new methods for improving the microdistribution of mAbs within the tumor are needed.

We demonstrated therapeutic effect of NIR-release, NIR-PIT and combination of NIR-PIT and NIR-release *in vitro* as shown in Fig. 1D. Moreover, we showed that the combination of NIR-PIT and NIR-drug release proved robust therapeutic effects on EGFR-expressing MDAMB468 tumors compared with NIR-PIT alone or NIR-release alone therapy as shown in Fig. 4. After the first NIR-PIT, additional CyEt-Pan-Duo can enter the treated tumor bed more deeply due to the greater permeability and penetration afforded by the SUPR effect which follows NIR-PIT (Fig. 2). There, additional APC bind homogeneously to the surviving fraction of cancer cells (6). Therefore, the second exposure to NIR light enhances the release of duocarmycin causing local cytotoxicity. On the other hand, when CyEt-Pan-Duo is used without prior NIR-PIT it tends to accumulate preferentially in the perivascular space with lower concentrations of duocarmycin reaching deeper into the tumor (Fig. 5).

CyEt-Pan-Duo achieved sufficient tumor TBRs as shown in Fig. 2, to be potentially practical for clinical application during surgical, endoscopic or trans-needle procedures. Efficient binding and distribution of the antibody are important for APCs to be effective as agents for NIR treatment. This also holds for antibody-toxin or antibody-drug conjugates since, to be effective, the drugs and toxins must be internalized after cell binding. Our results

demonstrated that once CyEt-Pan-Duo bound to target tumor cells it was internalized within 6 hours of incubation (Fig. 1). Moreover, following application of NIR light exposure, the 800 nm fluorescence intensity of the tumor was nearly completely extinguished, indicating duocarmycin release (16). These results suggest that CyEt-Pan-Duo has favorable characteristics as a NIR-releasing antibody-drug conjugate.

Cyanine-based antibody drug conjugate linkers could enable small molecule delivery with high precision through the combination of antibody targeting and NIR light mediated release. Light provides an external stimulus to precisely time and target the release of drugs (26, 27). Our data demonstrate that tumor growth was reduced and survival was prolonged significantly in the NIR-release alone group compared with the control group. As shown in Fig. 1D, the optimal cyanine conjugate, CyEt-Pan-Duo, displayed significant antitumor efficacy due to the release of duocarmycin after NIR light.

After the initial NIR-PIT, the subsequent SUPR effect permitted deeper penetration of still-circulating APCs into the tumor enabling them to bind uniformly to surviving cancer cells. A second light exposure thus, results in further cell killing (7). Thus, to maximize the effect of NIR-PIT after a single injection of pan-IR700 two sequential light exposures should be performed. Moreover, to obtain the maximal therapeutic effect from the combination of NIR-PIT and NIR-release, CyEt-Pan-Duo should maximally enter tumor cells with little background uptake. Fluorescence imaging of the tumor also showed that the skin uptake was still high up to one day of incubation (Fig. 2). Thus, we used 1 day of incubation with CyEt-Pan-Duo to achieve a reasonable TBR whereupon the 2nd NIR light exposure released duocarmycin from the CyEt-Pan-Duo. Thus, the 2nd shot of NIR light served two purposes, the first to activate pan-IR700 APCs that had reaccumulated in the tumor and the second to release duocarmycin from CyEt-Pan-Duo.

While the combination therapy with NIR-PIT and NIR-release showed highly selective cytotoxicity, and NIR light can be easily applied to superficial tumors, an obvious limitation is the inability to deliver NIR light to the tumor located deep in the tissue. Skin, fat and other organs will absorb NIR light before it reaches the tumor. There are several potential solutions to this problem. For instance, NIR light could be delivered to a tumor and to adjacent structures while the tissues are still exposed during a surgical resection, thus treating residual tumor in the tumor margin or in regional lymph nodes. Such procedures have been proposed in the past with PDT (28, 29); however, we believe that NIR-PIT would be much more effective with lower toxicity than PDT. Alternatively, fiber optic light probes could be placed within or nearby tumor using endoscopes, laparoscopes, catheters or image guided percutaneous needles. Recently, new type of cancer photo-therapy was also reported. Cancer cells expressing specific fluorescent proteins can be treated with exposure of ultra violet C (UVC) (30–33). However, the wavelength of UVC is shorter than that of NIR, therefore, UVC light does not penetrate deep into tissue. Furthermore, fluorescent proteins should be genetically transfected into cancer cells *in vivo*. Therefore, we think NIR-PIT would be technically simple and easy. Other caveat in this study is that subcutaneously-growing human tumors in immunodeficient mice do not sufficiently represent clinical cancer. Superior tumor models such as surgically orthotopic tumor model can clarify the pre-clinical effect of treatment (34, 35), yet surgical orthotopic injection requires highly trained

surgical skills and invasive methods. On the other hand, the cell injection model requires less advanced skills, and is less invasive, so we chose the cell injection model. We used anti-EGFR antibody, panitumumab, in both NIR-PIT and NIR-release. To some extent pan-IR700 may compete with CyEt-Pan-Duo for EGFR on the remaining cells after initial NIR light exposure (6, 7). As the result, additional binding of CyEt-Pan-Duo might be blocked by prior saturation with pan-IR700. Thus, it may be advantageous to study the effect of performing NIR-PIT with a different antibody than panitumumab. This experiment is planned for the future. Finally, repeated dosing of the APCs with repeated light exposures is likely to increase effectiveness (7, 36). Thus, it would be desirable to extend these studies to include multiple doses of the APCs and multiple NIR light exposures.

Conclusion

CyEt-Panitumumab-Duocarmycin degree of labeling 4, CyEt-Pan-Duo, accumulates in EGFR-expressing cancer cells and releases duocarmycin after NIR light exposure. Prior treatment with NIR-PIT results in improved microdistribution of CyEt-Pan-Duo and additive therapeutic responses in EGFR-expressing cancers. The combination of NIR-PIT and NIR-release is a promising candidate for the treatment of tumors and could be readily translated to humans.

Supplementary Material

Refer to Web version on PubMed Central for supplementary material.

Acknowledgments

Financial support

All authors were supported by the Intramural Research Program of the NIH, NCI, Center for Cancer Research (ZIA BC011513).

Abbreviations

ANOVA	one-way analysis of variance
APC	antibody-photo-absorber conjugate
BLI	bioluminescence imaging
DIC	differential interference contrast
EGFR	epidermal growth factor receptor
FDA	Food and Drug Administration
IR700	IRDye700DX
LED	light-emitting diode
mAb	monoclonal antibodies
NIR	near-infrared

OCT	optimal cutting temperature
PBS	phosphate buffered saline
PDT	photodynamic therapy
PI	propidium iodide
PIT	photoimmunotherapy
ROI	regions of interest
SEC	size-exclusion chromatography
SEM	standard error of mean
SDS-PAGE	sodium dodecyl sulfate-polyacrylamide gel electrophoresis
SUPR	super enhanced permeability and retention
TBR	target-to-background ratio
US	United States

References

1. Mitsunaga M, Ogawa M, Kosaka N, Rosenblum LT, Choyke PL, Kobayashi H. Cancer cell-selective in vivo near infrared photoimmunotherapy targeting specific membrane molecules. Nat Med. 2011; 17:1685–91. [PubMed: 22057348]
2. Ogawa M, Tomita Y, Nakamura Y, Lee MJ, Lee S, Tomita S, et al. Immunogenic cancer cell death selectively induced by near infrared photoimmunotherapy initiates host tumor immunity. Oncotarget. 2017; 8:10425–36. [PubMed: 28060726]
3. Kobayashi H, Watanabe R, Choyke PL. Improving conventional enhanced permeability and retention (EPR) effects; what is the appropriate target? Theranostics. 2013; 4:81–9. [PubMed: 24396516]
4. Sano K, Nakajima T, Choyke PL, Kobayashi H. Markedly enhanced permeability and retention effects induced by photo-immunotherapy of tumors. ACS Nano. 2013; 7:717–24. [PubMed: 23214407]
5. Sano K, Nakajima T, Choyke PL, Kobayashi H. The effect of photoimmunotherapy followed by liposomal daunorubicin in a mixed tumor model: a demonstration of the super-enhanced permeability and retention effect after photoimmunotherapy. Mol Cancer Ther. 2014; 13:426–32. [PubMed: 24356818]
6. Nagaya T, Nakamura Y, Sato K, Harada T, Choyke PL, Kobayashi H. Improved micro-distribution of antibody-photon absorber conjugates after initial near infrared photoimmunotherapy (NIR-PIT). J Control Release. 2016; 232:1–8. [PubMed: 27059723]
7. Mitsunaga M, Nakajima T, Sano K, Choyke PL, Kobayashi H. Near-infrared theranostic photoimmunotherapy (PIT): repeated exposure of light enhances the effect of immunoconjugate. Bioconjug Chem. 2012; 23:604–9. [PubMed: 22369484]
8. Luo S, Zhang E, Su Y, Cheng T, Shi C. A review of NIR dyes in cancer targeting and imaging. Biomaterials. 2011; 32:7127–38. [PubMed: 21724249]
9. Weissleder R. A clearer vision for in vivo imaging. Nat Biotechnol. 2001; 19:316–7. [PubMed: 11283581]
10. Ballou B, Ernst LA, Waggoner AS. Fluorescence imaging of tumors in vivo. Curr Med Chem. 2005; 12:795–805. [PubMed: 15853712]

11. Gorka AP, Nani RR, Schnermann MJ. Cyanine polyene reactivity: scope and biomedical applications. Org Biomol Chem. 2015; 13:7584–98. [PubMed: 26052876]
12. Levitus M, Ranjit S. Cyanine dyes in biophysical research: the photophysics of polymethine fluorescent dyes in biomolecular environments. Q Rev Biophys. 2011; 44:123–51. [PubMed: 21108866]
13. Mishra A, Behera RK, Behera PK, Mishra BK, Behera GB. Cyanines during the 1990s: A Review. Chem Rev. 2000; 100:1973–2012. [PubMed: 11749281]
14. Gorka AP, Schnermann MJ. Harnessing cyanine photooxidation: from slowing photobleaching to near-IR uncaging. Curr Opin Chem Biol. 2016; 33:117–25. [PubMed: 27348157]
15. Solomek T, Wirz J, Klan P. Searching for Improved Photoreleasing Abilities of Organic Molecules. Acc Chem Res. 2015; 48:3064–72. [PubMed: 26569596]
16. Nani RR, Gorka AP, Nagaya T, Yamamoto T, Ivanic J, Kobayashi H, et al. In Vivo Activation of Duocarmycin-Antibody Conjugates by Near-Infrared Light. ACS Cent Sci. 2017; 3:329–37. [PubMed: 28470051]
17. Mitsunaga M, Nakajima T, Sano K, Kramer-Marek G, Choyke PL, Kobayashi H. Immediate in vivo target-specific cancer cell death after near infrared photoimmunotherapy. BMC Cancer. 2012; 12:345. [PubMed: 22873679]
18. Sato K, Watanabe R, Hanaoka H, Harada T, Nakajima T, Kim I, et al. Photoimmunotherapy: comparative effectiveness of two monoclonal antibodies targeting the epidermal growth factor receptor. Mol Oncol. 2014; 8:620–32. [PubMed: 24508062]
19. Graff CP, Wittrup KD. Theoretical analysis of antibody targeting of tumor spheroids: importance of dosage for penetration, and affinity for retention. Cancer Res. 2003; 63:1288–96. [PubMed: 12649189]
20. Jain RK, Baxter LT. Mechanisms of heterogeneous distribution of monoclonal antibodies and other macromolecules in tumors: significance of elevated interstitial pressure. Cancer Res. 1988; 48:7022–32. [PubMed: 3191477]
21. Thurber GM, Schmidt MM, Wittrup KD. Antibody tumor penetration: transport opposed by systemic and antigen-mediated clearance. Adv Drug Deliv Rev. 2008; 60:1421–34. [PubMed: 18541331]
22. Fujimori K, Covell DG, Fletcher JE, Weinstein JN. A modeling analysis of monoclonal antibody percolation through tumors: a binding-site barrier. J Nucl Med. 1990; 31:1191–8. [PubMed: 2362198]
23. Juweid M, Neumann R, Paik C, Perez-Bacete MJ, Sato J, van Osdol W, et al. Micropharmacology of monoclonal antibodies in solid tumors: direct experimental evidence for a binding site barrier. Cancer Res. 1992; 52:5144–53. [PubMed: 1327501]
24. van Osdol W, Fujimori K, Weinstein JN. An analysis of monoclonal antibody distribution in microscopic tumor nodules: consequences of a “binding site barrier”. Cancer Res. 1991; 51:4776–84. [PubMed: 1893370]
25. Weinstein JN, van Osdol W. Early intervention in cancer using monoclonal antibodies and other biological ligands: micropharmacology and the “binding site barrier”. Cancer Res. 1992; 52:2747s–51s. [PubMed: 1563006]
26. Gorka AP, Nani RR, Zhu J, Mackem S, Schnermann MJ. A near-IR uncaging strategy based on cyanine photochemistry. J Am Chem Soc. 2014; 136:14153–9. [PubMed: 25211609]
27. Nani RR, Gorka AP, Nagaya T, Kobayashi H, Schnermann MJ. Near-IR Light-Mediated Cleavage of Antibody-Drug Conjugates Using Cyanine Photocages. Angew Chem Int Ed Engl. 2015; 54:13635–8. [PubMed: 26403799]
28. Hiroshima Y, Maawy A, Zhang Y, Sato S, Murakami T, Yamamoto M, et al. Fluorescence-guided surgery in combination with UVC irradiation cures metastatic human pancreatic cancer in orthotopic mouse models. PLoS One. 2014; 9:e99977. [PubMed: 24924955]
29. Pass HI, Temeck BK, Kranda K, Thomas G, Russo A, Smith P, et al. Phase III randomized trial of surgery with or without intraoperative photodynamic therapy and postoperative immunochemotherapy for malignant pleural mesothelioma. Ann Surg Oncol. 1997; 4:628–33. [PubMed: 9416409]

30. Kimura H, Lee C, Hayashi K, Yamauchi K, Yamamoto N, Tsuchiya H, et al. UV light killing efficacy of fluorescent protein-expressing cancer cells in vitro and in vivo. J Cell Biochem. 2010; 110:1439–46. [PubMed: 20506255]

31. Momiyama M, Suetsugu A, Kimura H, Kishimoto H, Aki R, Yamada A, et al. Fluorescent proteins enhance UVC PDT of cancer cells. Anticancer Res. 2012; 32:4327–30. [PubMed: 23060554]

32. Momiyama M, Suetsugu A, Kimura H, Kishimoto H, Aki R, Yamada A, et al. Imaging the efficacy of UVC irradiation on superficial brain tumors and metastasis in live mice at the subcellular level. J Cell Biochem. 2013; 114:428–34. [PubMed: 22961687]

33. Tsai MH, Aki R, Amoh Y, Hoffman RM, Katsuoka K, Kimura H, et al. GFP-fluorescence-guided UVC irradiation inhibits melanoma growth and angiogenesis in nude mice. Anticancer Res. 2010; 30:3291–4. [PubMed: 20944099]

34. Hoffman RM. Orthotopic metastatic mouse models for anticancer drug discovery and evaluation: a bridge to the clinic. Invest New Drugs. 1999; 17:343–59. [PubMed: 10759402]

35. Hoffman RM. Patient-derived orthotopic xenografts: better mimic of metastasis than subcutaneous xenografts. Nat Rev Cancer. 2015; 15:451–2. [PubMed: 26422835]

36. Nagaya T, Sato K, Harada T, Nakamura Y, Choyke PL, Kobayashi H. Near Infrared Photoimmunotherapy Targeting EGFR Positive Triple Negative Breast Cancer: Optimizing the Conjugate-Light Regimen. PLoS One. 2015; 10:e0136829. [PubMed: 26313651]

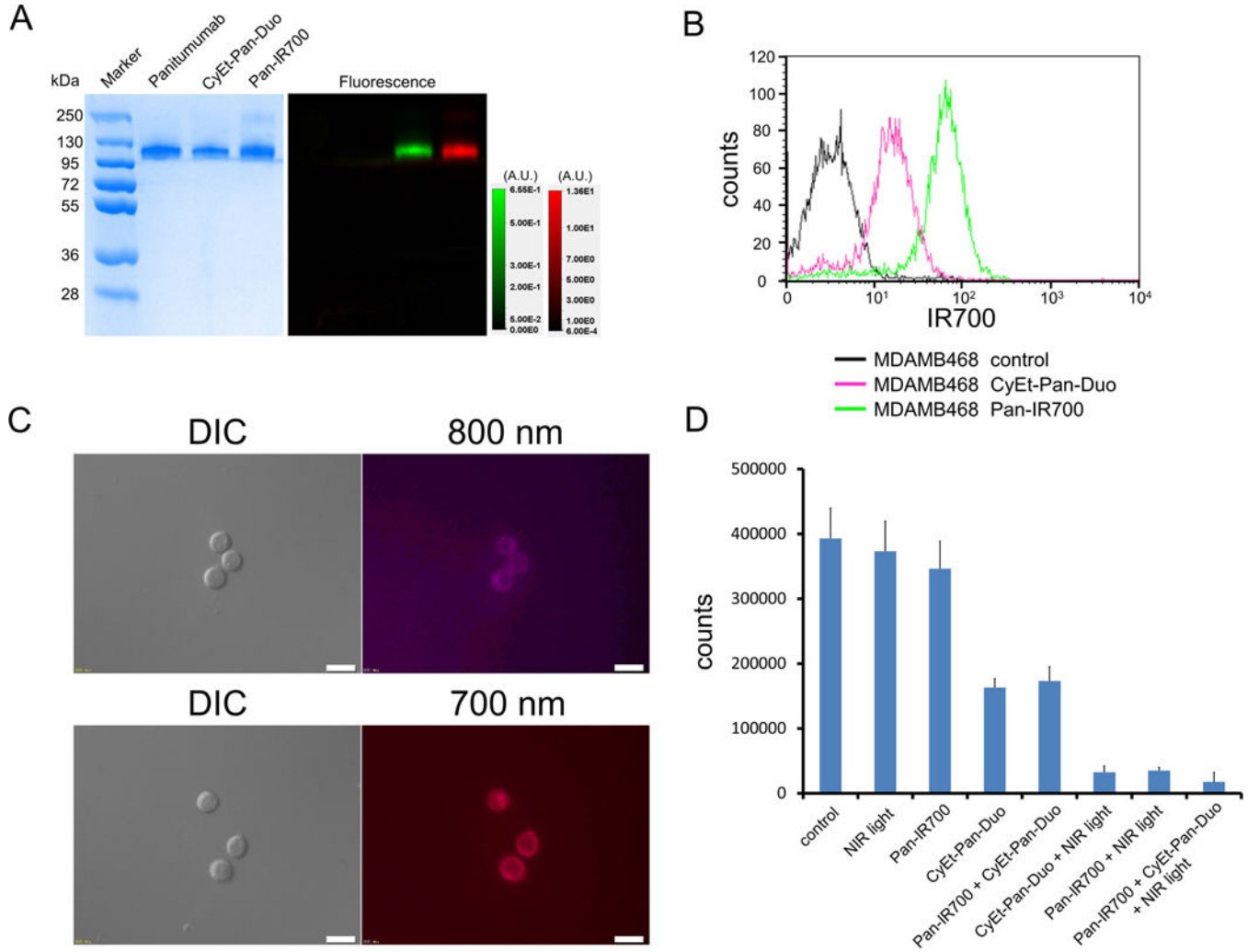

Figure 1. Characterization of pan-IR700 and CyEt-Pan-Duo on MDAMB468-luc cell

(A) Validation of pan-IR700 and CyEt-Pan-Duo by SDS-PAGE (left: Colloidal Blue staining, right: fluorescence). Diluted panitumumab was used as a control. (B) Specific binding of pan-IR700 and CyEt-Pan-Duo in EGFE-expressing MDAMB468-luc cells was evaluated by FACS. After 6 h of pan-IR700 and CyEt-Pan-Duo incubation, MDAMB468-luc cells showed high fluorescence signal. (C) Differential interference contrast (DIC) and fluorescence microscopy images of MDAMB468-luc cells after incubation with either pan-IR700 or CyEt-Pan-Duo for 6 h. High fluorescence intensities were shown in MDAMB468-luc cells (upper: CyEt-Pan-Duo, lower: Pan-IR700). Scale bars = 20 μm. (D) Cell counts after each treatment were measured using a cell counter. Mild cell killing was shown in CyEt-Pan-Duo and pan-IR700 + CyEt-Pan-Duo groups. Greater cytotoxicity was shown in three treatment groups with NIR light exposure especially in the combination therapy group. There was no cytotoxicity associated with NIR light alone and pan-IR700 alone.

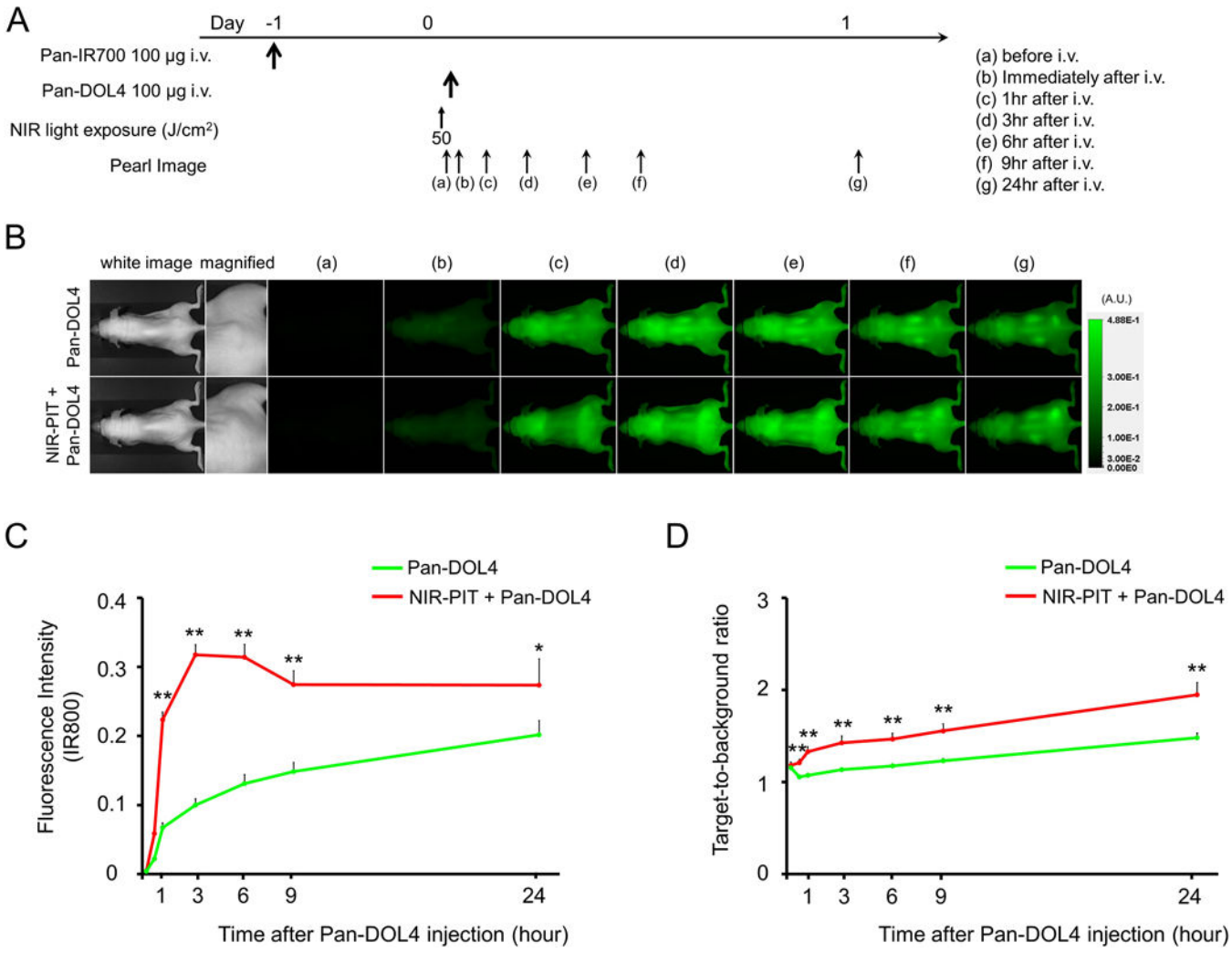

Figure 2. *In vivo* 800 nm fluorescence imaging studies using CyEt-Pan-Duo

(A) The regimen of imaging is shown. Fluorescence images were obtained at each time point as indicated. (B) *In vivo* 800 nm fluorescence real-time imaging of tumor-bearing mice (right dorsum). The tumor showed high fluorescence intensity after CyEt-Pan-Duo injection and the 800 nm intensity in both CyEt-Pan-Duo only tumor and NIR-PIT + CyEt-Pan-Duo tumor. The 800 nm fluorescence signal was higher in NIR-PIT + CyEt-Pan-Duo group compared to CyEt-Pan-Duo only group. (C) Quantitative analysis of 800 nm fluorescence intensities in tumors (n = 10). The 800 nm fluorescence intensity in NIR-PIT + CyEt-Pan-Duo tumors showed continuously high intensities within 1 day after injection. On the other hand, the 800 nm fluorescence intensity in the CyEt-Pan-Duo only tumors increased gradually within 1 day. The 800 nm fluorescence intensities were significantly higher in NIR-PIT + CyEt-Pan-Duo group compared to CyEt-Pan-Duo only group at the most time points (**, $p < 0.01$ at 1, 3, 6, and 9 hour, $p < 0.05$ at 24 hour, by Mann-Whitney-U test). (D) Quantitative analysis of TBR in tumors (n = 10). TBR increased gradually within 24 hour in both CyEt-Pan-Duo only tumors and NIR-PIT + CyEt-Pan-Duo tumors. TBRs were significantly higher in NIR-PIT + CyEt-Pan-Duo group compared to CyEt-Pan-Duo only group at all time points (**, $p < 0.01$, by Mann-Whitney-U test).

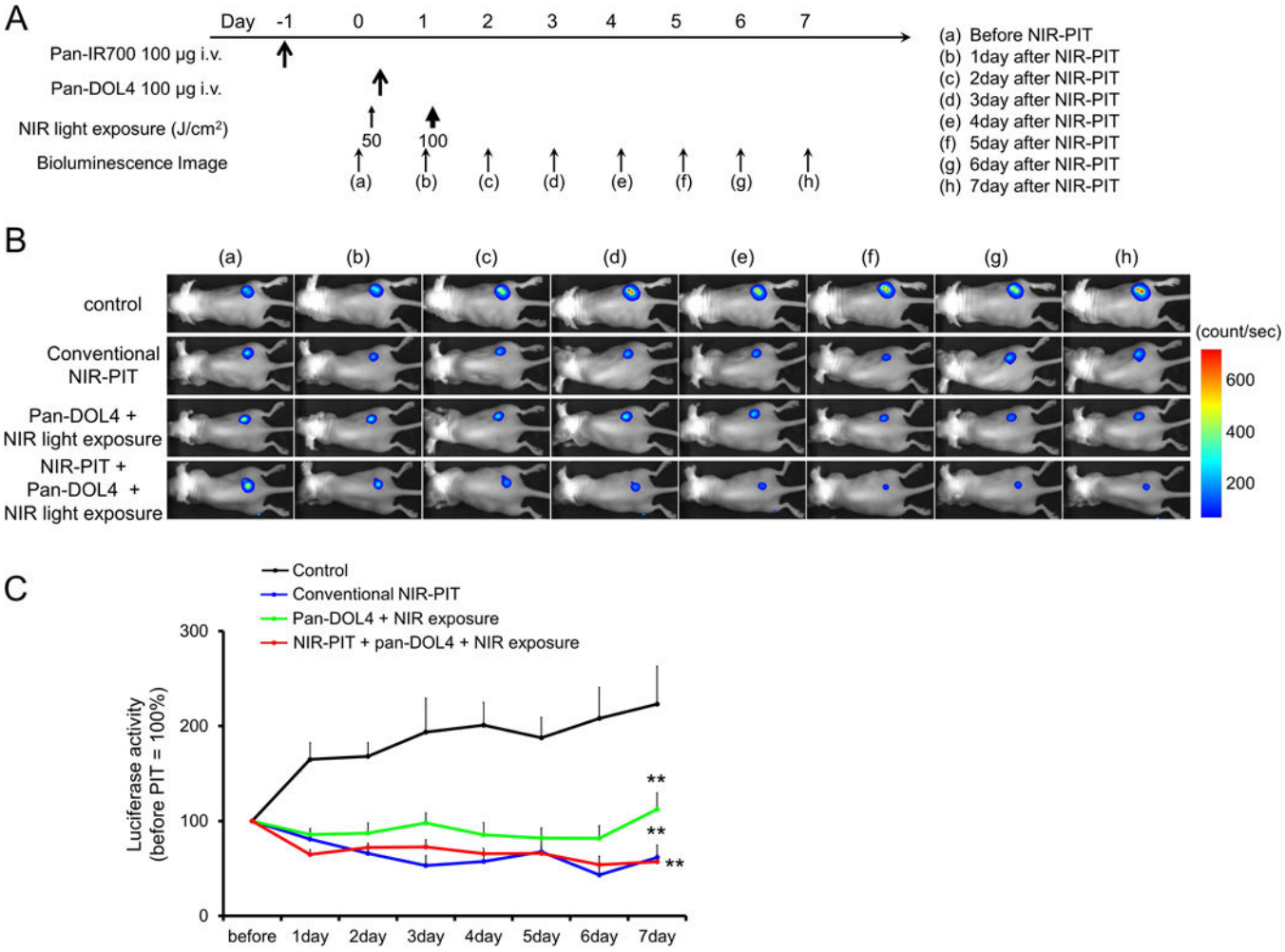

Figure 3. ***In vivo*** **treatment effect of combination therapy with NIR-PIT and NIR-release using luciferase activity**

(A) Therapeutic regimen. Bioluminescence images were obtained at each time point as indicated. (B) *In vivo* bioluminescence images of tumor bearing mice in response to treatment. Before treatment, tumors were approximately the same size and exhibited similar bioluminescence. All treated tumors (NIR-PIT, NIR-release, and NIR-PIT + NIR-release) showed decreasing luciferase activity after treatment. (C) Quantitative luciferase activity (before NIR-PIT is set to 100) showed a significant decrease in all treatment groups ($n \geqq 10$, $^{**}p < 0.01$ vs. control group, by Tukey's test with ANOVA). Luciferase activity of tumor in control group showed an increase due to rapid tumor growth.

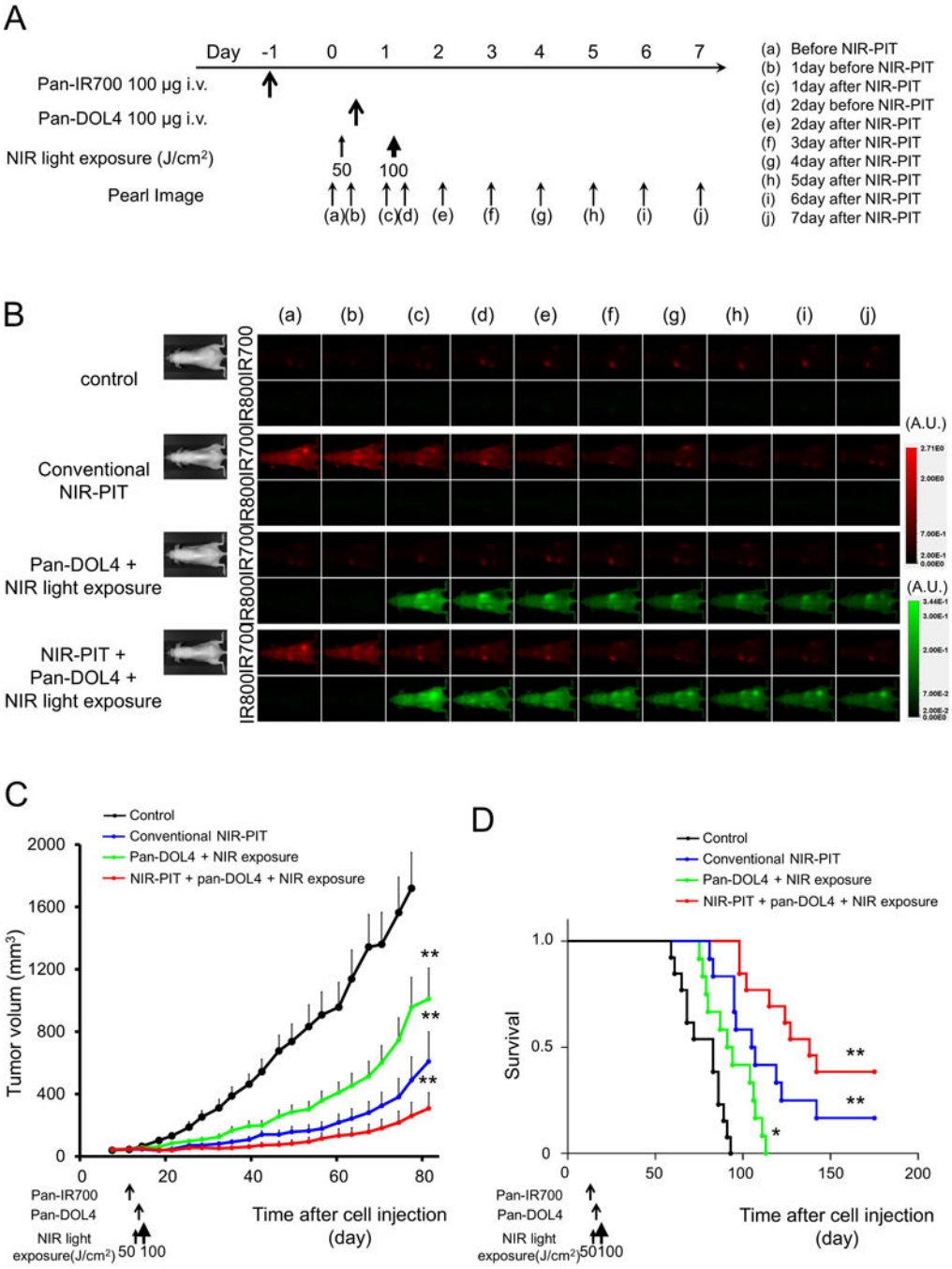

Figure 4. *In vivo* treatment effect of combination therapy with NIR-PIT and NIR-release

(A) Therapeutic regimen. Fluorescence images were obtained at each time point as indicated. (B) *In vivo* fluorescence real-time images of tumor bearing mice in response to treatment. The tumor treated by NIR-PIT showed decreasing 700 nm fluorescence signal after NIR-PIT. One day after injection of CyEt-Pan-Duo, the tumors in NIR-PIT + NIR-release group showed higher CyEt-Pan-Duo fluorescence intensity than did the tumor in NIR-release group. Immediately after exposure to 100 J/cm^2 of NIR light, tumor CyEt-Pan-Duo fluorescence signal strongly decreased due to photo-release. After photo-release, CyEt-

Pan-Duo fluorescence signal gradually increased over the following days in both tumors in NIR-release group and NIR-PIT + NIR-release group. The re-accumulation of CyEt-Pan-Duo was strongly shown in NIR-PIT + NIR-release tumor compared with NIR-release tumor. (C) Tumor growth was significantly inhibited in all treatment groups compared with the control group (n ≧ 10, **, $p < 0.001$, by Tukey's test with ANOVA). Tumor growth of NIR-PIT + NIR-release group was also significantly improved compared with NIR-release only group (*, $p < 0.05$, by Tukey's test with ANOVA). (D) Significantly prolonged survival was observed in all treatment groups compared with control group (n ≧ 10, *, $p < 0.05$ for NIR-release group, **, $p < 0.01$ for NIR-PIT group and NIR-PIT + NIR-release group, by Tukey's test with ANOVA). Survival of NIR-PIT group was significantly improved compared with NIR-release only group (***, $p < 0.01$, by Gehan-Breslow-Wilcoxon test). Furthermore, significantly prolonged survival was also achieved in NIR-PIT + NIR-release group compared with NIR-PIT group (****, $p < 0.05$, by Gehan-Breslow-Wilcoxon test).

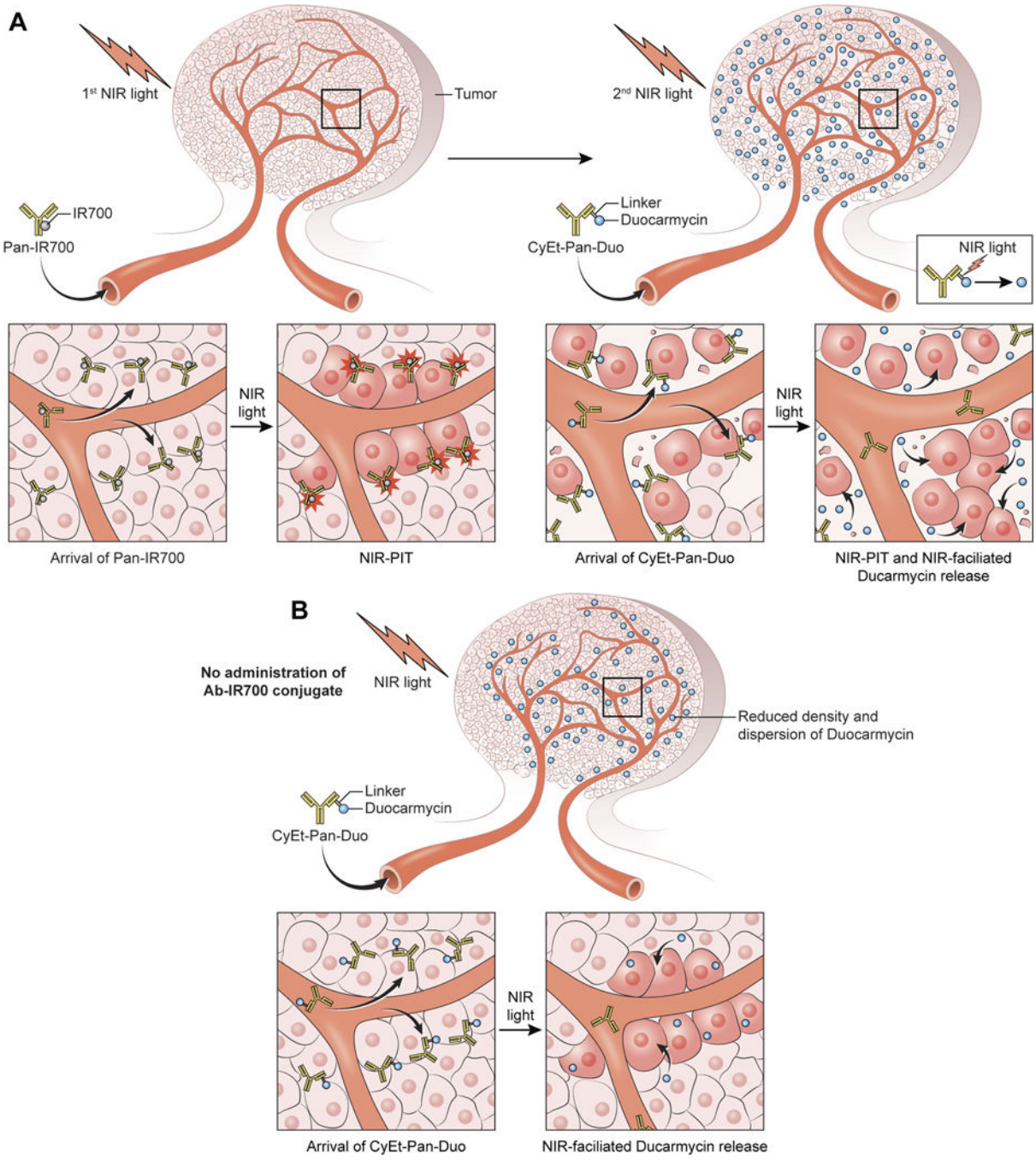

Figure 5. Schematic presentation of the combination therapy with NIR-PIT and NIR-release

(A) Pan-IR700 is saturated on antigen-positive cells in the immediate perivascular space. 1st NIR light induces a profound perivascular cell death leading to the massive leakage of additional CyEt-Pan-Duo into the tumor bed with greater permeability and penetration. There, CyEt-Pan-Duo binds homogeneously to the surviving fraction of cancer cells. 2nd NIR-light can effectively release duocarmycin from CyEt-Pan-Duo. (B) CyEt-Pan-Duo-only

results in saturation of antigen-positive cells in the immediate perivascular space reducing the concentration and dispersion of duocarmycin.